

# Lora Communication System for Early Detection and Monitoring of Water Toxicity in Floating Net Cages

Rahmafadilla<sup>1</sup>, Indrarini Dyah Irawati<sup>2,\*</sup>, Mochammad Fahru Rizal<sup>3</sup>, Siti Sarah Maidin<sup>4</sup>

<sup>1,2,3</sup>*School of Applied Science, Telkom University, Bandung, Indonesia*

<sup>4</sup>*Faculty of Data Science and Information technology, INTI International University, Negeri Sembilan, Malaysia*

(Received: 25 February 2025; Revised: 25 April 2025; Accepted: 25 June 2025; Available online: 25 August 2025)

## Abstract

Floating Net Cages/ Keramba Jaring Apung (KJA) are at risk of polluting the air, which can affect fish farming. Therefore, an early monitoring system is needed that can measure air quality such as temperature, pH, and dissolved oxygen (DO) in real-time. This system utilizes the LoRa RFM95W module to wirelessly transmit environmental data from sensors installed on the cages, which continuously monitor water quality parameters such as temperature, pH, and DO in real-time. The data obtained is then processed to monitor changes in water toxicity in real-time, allowing early detection of potential threats to the ecosystem. Tests were conducted at distances of 50m, 180m, 300m, 340m, and 440m. The results showed that the system worked well up to a distance of 300m with RSSI values between -85 dBm to -120 dBm and SNR more than 2 dB. However, at distances of 340m and 440m, the signal decreased and the delay increased. At a depth of 340m, only one experiment was successful with RSSI -134 dBm and SNR -6 dB, while at a depth of 440m, only a few experiments were successful with RSSI between -122 dBm to -132 dBm and SNR between 1 dB to -6 dB. The prototype system successfully transmitted real-time air quality data to a web-based monitoring center. Data from the sensors were sent via the LoRa network to a central server for further monitoring.

**Keywords:** Floating Net Cages (KJA), LoRa RFM95W, RSSI, Delay, SNR, Water Quality, Marine conservation, Product Innovation

## 1. Introduction

Indonesia has enormous potential for fisheries resources, both from the capture fisheries and aquaculture sectors. Based on data from the Indonesian Central Statistics Agency (BPS) in 2022, this sector recorded a growth in the fisheries sector of 5.45% [1]. Fish cultivation itself is not limited to sea waters, but is also growing rapidly in freshwater such as lakes, reservoirs, and rivers [2]. One of the cultivation methods that is widely applied in lakes and reservoirs is the Floating Net Cage (KJA) [3]. The KJA system was first implemented in 1974 in the Jatiluhur area, West Java [4].

The KJA is a means of raising fish whose frame is made of bamboo, wood, PVC pipe or square-shaped iron which is equipped with nets and floats so that the container remains floating in the water [5]. This system makes it easier to feed and monitor the condition of the fish, thus supporting more natural growth and more efficient cultivation management [6]. However, fish farming with the KJA system also has a negative impact on the environment, especially related to water pollution due to the accumulation of organic matter from uneaten feed, feces, and fish urine. This accumulation has the potential to worsen water quality and trigger eutrophication, which is an increase in organic matter levels that can cause a decrease in dissolved oxygen levels [7]. This condition has an impact on the survival of fish and other organisms in the aquatic ecosystem. The pH value that is considered neutral for waters ranges from 6.5 to 8.5 [8].

Several reports indicate that hundreds of fish in KJA experienced sudden death due to poisoning, with a total of around 15 tons of fish affected [9], [10]. This condition shows the importance of a more effective water quality monitoring system to maintain the balance of the aquatic ecosystem and prevent economic losses for fish farmers [11]. Various methods have been developed to increase the effectiveness of water quality monitoring, ranging from conventional methods to the use of digital technology. In Research [12], combined 3G technology with Android operating system

\*Corresponding author: Indrarini Dyah Irawati ([indrarini@telkomuniversity.ac.id](mailto:indrarini@telkomuniversity.ac.id))

DOI: <https://doi.org/10.47738/jads.v6i3.787>

This is an open access article under the CC-BY license (<https://creativecommons.org/licenses/by/4.0/>).

© Authors retain all copyrights

for water quality monitoring. However, 3G networks have several limitations, such as continuous data subscription costs, uneven signal coverage in remote areas, and high-power consumption, which can complicate the operation of devices in the field. In addition, in the research [13], conventional methods that rely on WiFi and GSM have several limitations. For example, limited WiFi coverage, high operational costs for GSM, and high-power consumption in both methods. One effective solution that can be implemented is the use of Internet of Things (IoT) technology combined with Long Range (LoRa) communication [14]. LoRa is a wireless communication technology that enables long-distance data transmission with low power consumption [15], [16], [17], [18]. This technology is capable of sending data up to 22 km in line of sight (LOS) conditions at sea using a low-cost off-the-shelf rubber duck antenna. With a higher gain antenna, the range can increase to 28 km [19]. LoRa technology is very suitable for application in aquatic environments such as lakes and reservoirs, where communication network infrastructure is often limited [20].

In research [21], water quality has been studied using a communication module, but only focused on sensor data that reaches the receiver and is monitored on the web. This study did not measure the distance to the LoRa used and did not include the distance between the LoRa node and the LoRa gateway. In research [22], the performance of LoRa-SX1278 as a LoRa gateway was tested against the distance at LoS and NLoS. The packets that were successfully received at the last LoS were at a distance of 150 meters, and NLoS at 50 meters.

Unlike previous studies, this study specifically focuses on determining the optimal distance for placing LoRa nodes and LoRa gateways by considering technical parameters such as RSSI, delay, and SNR. By measuring these parameters, this study aims to obtain the best configuration in the placement of LoRa devices so that data communication remains stable, efficient, and suitable for application in monitoring water quality in lakes and reservoirs. With this approach, the IoT-based water quality monitoring system can be further optimized, both in terms of communication range and the accuracy of the data sent, thus supporting the sustainability of fish farming in open waters.

## 2. Literature Review

### 2.1. LoRa

LoRa is a wireless communication technology developed by Semtech for IoT applications in long-distance data transmission with low power consumption [23]. LoRa has attracted significant attention from students and researchers due to its off-the-shelf hardware, which can be customized to improve energy efficiency and link-level performance. LoRa uses Chirp Spread Spectrum (CSS) based spread spectrum modulation technique that enables long-range communication with minimal interference [24]. LoRa operates on the 433 MHz, 868 MHz, and 915 MHz frequencies, which utilize the unlicensed ISM band. The maximum period of time a LoRa device is allowed to occupy an ISM band is expressed in Duty Cycle (DC). Duty cycle ranges from 0.1% to 10%, the maximum duty cycle limit allowed for LoRa devices in the 433 MHz ISM band is 10%. This means that LoRa devices should not use the radio channel for more than 8640 seconds in a day. Due to this duty cycle limitation, the device will enter a sleep period after sending a data frame. As a result, there will be a delay between two consecutive LoRa frames [25].

### 2.2. Received Signal Strength Indicator (RSSI)

RSSI is an indicator in wireless communication in a certain range of values, depending on the type of signal (indoor or outdoor). RSSI is the remaining signal strength plus interference at the receiver side, taking into account attenuation caused by connectors, cables, and signal losses along the path, as well as the gain of the Node and Gateway antennas. RSSI serves as an effective metric for determining the position of a Node. Since RSSI intrinsically reflects signal loss which is directly affected by distance, RSSI allows a natural method to estimate the distance between a Node and a gateway, assuming the path loss model is known. Once the distance is estimated, the gateway position can be determined using techniques such as angle measurement or lateration [26]. The RSSI value of a cellular receiver is preceded by a negative sign, and its unit is dBm. RSSI performance is affected by factors such as path loss and environment. When path loss increases, RSSI will decrease at the receiver. The long distance between the transmitter and receiver also causes RSSI to decrease. Periodic maintenance for the overall communication system must be implemented to avoid RSSI deficiencies [27].

### 2.3. Signal to Noise Ratio (SNR)

The SNR is the ratio between the desired signal power and the noise power, and is used as a standard for measuring signal quality in communication systems. SNR is an important component of communication; the SNR value is collected with the RSSI value for each reference point [28]. The higher the SNR value, the stronger and clearer the signal is compared to noise, while a low SNR indicates a weaker signal, which is difficult to distinguish from noise. SNR is usually expressed in decibels (dB) and plays an important role in determining the reliability and performance of a communication system [29]. By understanding and optimizing SNR values, network operators can improve transmission efficiency, extend communication coverage, and reduce error rates in data transmission, which ultimately improves the quality of service in various wireless communication applications.

### 2.4. Delay

Delay is the time it takes for a data packet to travel from source to destination. Delay can be affected by distance, physical media, traffic congestion, or long processing times. Delay in LoRa refers to the time it takes for data to travel from sender to receiver [30]. This delay is affected by several main factors, such as Spreading Factor (SF), Bandwidth (BW), Duty Cycle, interference, and environmental conditions. A higher SF enables long-distance communication but increases transmission time, while a lower SF speeds up data delivery but reduces range [31], [32]. Duty Cycle also affects delay because it limits transmission time in a certain period. For example, with a Duty Cycle of 1%, a device can only send data for 1 second and then has to wait 99 seconds before sending again, which causes significant delay [33], [34]. Higher BW speeds up transmission but consumes more power, while lower BW increases signal sensitivity but slows down delivery [35]. Interference from other devices and physical obstacles such as buildings and trees can also increase delay because they cause signal reflection or attenuation. To reduce delay, parameters such as SF, BW, and transmission power need to be optimized according to application needs. With the right setup, LoRa communications can be faster and more efficient, especially in IoT applications that require real-time responses.

$$T_{packet} = SF \cdot \frac{PayloadSize}{BW} + T_{overhead} \quad (1)$$

$T_{packet}$  = packet transmission time;  $SF$  = Spreading factor;  $PayloadSize$  = Data length;  $BW$  = Bandwidth (Hz);  $T_{overhead}$  = Overhead time

The delay formula highlights the influence of parameters such as SF, BW, and payload size on transmission latency. By expressing this relationship mathematically, the paper clarifies why higher SF (used for longer distances) results in longer delays, even when the payload remains constant. This formula helps explain why the observed delays increase beyond 180m and peak at 340m. Practitioners can use this equation to calculate expected delays under different configurations, enabling them to balance between range and responsiveness depending on application needs.

### 2.5. Fresnel Zone and Path Loss

The Fresnel Zone radius formula is critical in understanding why signal strength fluctuates significantly at certain distances in the experiment, particularly at 340m and 440m. The Fresnel Zone represents the elliptical region between the transmitter and receiver through which the majority of the signal energy travels. Any obstruction within this zone (such as buildings, trees, or terrain) causes diffraction and attenuation, weakening the signal and increasing noise levels. In the experiment, the drastic degradation at 340m can be attributed to a fully obstructed Fresnel Zone, corresponding to a Non-Line of Sight (NLoS) condition. At 440m, although the direct path remains partially blocked, the Near-Line of Sight (nLoS) configuration allows some signal components to reach the receiver, explaining the slight improvement in RSSI and SNR observed beyond 340m. The Fresnel Zone radius equation quantifies this zone and enables engineers to calculate the required clearance height at specific distances and frequencies to minimize obstruction-related losses. For example, at 915 MHz and a total link distance of 300m, the first Fresnel Zone radius at midpoint is approximately 2.8 meters, highlighting how even relatively low obstructions can significantly impact link quality.

$$r = \sqrt{\frac{n\lambda d_1 d_2}{d_1 + d_2}} \quad (2)$$

$$PL(d) = PL(d_0) + 10n \log_{10} \left( \frac{d}{d_0} \right) + X_\sigma \quad (3)$$

The log-distance path loss model further contextualizes how distance and environmental factors contribute to the observed signal degradation. This model accounts for the inverse-square law of free-space propagation and adjusts it for real-world conditions through the path loss exponent  $n$ , which is higher in obstructed or urban environments. The addition of the stochastic term  $X_\sigma$  captures the random variability due to shadowing and multi-path fading. Applying this formula in the experiment clarifies why RSSI declined steadily from -94.7 dBm at 50m to -134 dBm at 340m: each doubling of distance increases path loss by approximately  $6n$  dB in free space (assuming  $n \approx 2$ ) and even more in obstructed environments where  $n$  can reach 3–4. In summary, combining these two theoretical tools (the Fresnel Zone radius to assess clearance requirements and the log-distance path loss to predict attenuation) provides a rigorous explanation of the empirical trends. This also underscores the importance of proper antenna placement and environment-aware planning to maintain robust communication links in IoT deployments.

### 3. Research Methods

The research method used in this study follows an experimental approach with direct testing in the lake water environment at the floating net cage location to build an effective LoRa communication system in early monitoring of lake water toxicity levels in floating net cages. This system utilizes a LoRa module to wirelessly transmit environmental data from sensors installed on the cages, which measure water quality parameters. The data obtained is then processed to monitor changes in water toxicity in real-time, allowing early detection of potential threats to the ecosystem. The main focus of this research is to evaluate the performance of the LoRa communication system in transmitting data efficiently and reliably, in order to improve environmental condition monitoring at fish farming sites.

#### 3.1. Hardware Components

The tap device components used in this study are ESP32, LoRa RFM95 and other sensor parameters. These components were carefully selected because of their affordable price, compatibility, and ability to work efficiently in the proposed system. The main part of this system is ESP32, a microcontroller developed by Espressif Systems as the successor to ESP8266. The main advantage of ESP32 lies in the integration of Wi-Fi and Bluetooth, making it very suitable for IoT applications. In addition, ESP32 has low power consumption, affordable cost, and more complex features than its predecessors, making it an ideal choice for projects with broader and more flexible wireless communication needs [36].

ESP32 acts as the main controller that processes data from various sensors, such as DS18B20 temperature sensor, pH sensor, and DO sensor, then sends and receives data through the LoRa module. Meanwhile, the LoRa RFM95W Module is a LoRa communication module that offers ultra-long-distance communication with high interference immunity and low power consumption with a sensitivity of more than -140dbm and a power amplifier of +20dbm. The RFM95W has a variety of bandwidth and spreading factor options, allowing users to customize performance according to application needs [37]. The technical specifications of the RFM95W module can be seen in [table 1](#). In addition, this module is designed for energy efficiency, with low power consumption in both receiving and operating modes. Despite its relatively low data rate, LoRa is very suitable for remote monitoring applications because it can transmit data within a radius of several kilometers with minimal power.

**Tabel 1.** RFM95W Module Specifications [37]

Frequency Band	868/915MHz
Spreading Factor	6-12
Bandwidth	125 – 500 kHz
Effective Bitrate	.293 – 37.5 kbps
Estimated Sensitivity	-111 to -136 dBm

[Table 2](#) provides the technical specifications of the sensors used in the system, complementing the previously detailed RFM95W module. It is crucial to include this table because the performance of the system also depends on the precision and sensitivity of these sensors. By presenting the range, accuracy, and resolution of the temperature, pH, and DO

sensors, the readers gain a better understanding of how the data collected reflects the true environmental conditions of the water.

**Table 2.** Sensor Specifications

Sensor	Parameter Measured	Range	Accuracy	Resolution
DS18B20 Temperature	Water Temperature	-55°C to +125°C	±0.5°C	0.0625°C
Analog pH Sensor	Water pH	0 to 14 pH	±0.1 pH	0.01 pH
DO	DO Concentration	0 to 20 mg/L	±0.3 mg/L	0.1 mg/L

Including the sensor specifications allows readers to evaluate the reliability of the monitoring system. For example, the DO sensor with an accuracy of ±0.3 mg/L ensures that the observed oxygen fluctuations are real and not artifacts of poor measurement. Furthermore, the narrow resolution of the DS18B20 temperature sensor (0.0625°C) enables the detection of even small changes in water temperature, which is significant for assessing water toxicity risks.

In this study, RFM95W is used to transmit and receive data from ESP32 via LoRa network, enabling real-time monitoring of lake water quality without relying on communication infrastructure such as Wi-Fi or cellular networks. Once the data is received, it is forwarded to a database for further storage and analysis. The combination of ESP32 and LoRa RFM95W in this system enables efficient data collection and transmission, making it an ideal solution for IoT-based environmental monitoring.

### 3.2. System Block Diagram

The system shows the LoRa communication architecture used for water quality monitoring in Floating Net Cages (KJA). The system block diagram in figure 1 illustrates the interconnected components in an IoT based monitoring system that utilizes LoRa technology to transmit data wirelessly with low power and wide range. This system consists of several nodes equipped with sensors to collect KJA data. Data collected by the sensors is processed by a microcontroller which then sends the information wirelessly using the LoRa RFM95W module to the LoRa Gateway.

The LoRa Gateway receives radio frequency signals from the nodes, then forwards the data to a server via a Wi-Fi/internet network connected via a router [38]. The server plays a role in storing data centrally and allows users to access and analyze data at any time. The stored data can be visualized in the form of graphs or tables via a website or application, so that users can monitor KJA conditions in real-time. With this system, water quality monitoring can be carried out remotely and continuously, allowing early detection of changes in environmental parameters that can have a negative impact on aquatic ecosystems. If anomalies or indications of water toxicity are found, users can immediately take mitigation steps to prevent further losses.

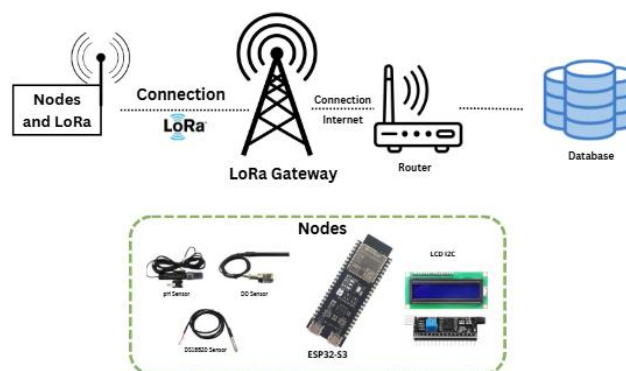


**Figure 1.** System Blok Diagram

### 3.3. Lora Communication System Workflow Diagram

The system workflow diagram in figure 2 illustrates the process of automatic data collection using LoRa technology. This process begins with the initialization of the tool, where the LoRa device and sensors are activated and ready to collect data. After initialization is complete, the system will read data from each sensor node installed in the KJA. After the sensor data is collected, the next step is to ensure that the LoRa Transmitter receives data from the sensor node. If



the data is not received, the system will return to the data reading process to try again. However, if the data is successfully received, the data will be sent directly to the LoRa Gateway via long-range wireless communication using the LoRaWAN protocol.

The LoRa Gateway is tasked with collecting data from various nodes and then forwarding it to the server via a Wi-Fi connection or internet network [38]. The collected data will be stored in a database, which functions as a data storage center for further monitoring and analysis purposes. After the data is stored, the system will display information on the website and mobile application, allowing users to monitor water quality in real-time. In addition, the system can also send automatic notifications to user devices, especially if there are significant changes in water quality parameters. In this way, users can immediately take mitigation steps to maintain the KJA ecosystem optimally and prevent negative impacts due to water toxicity.

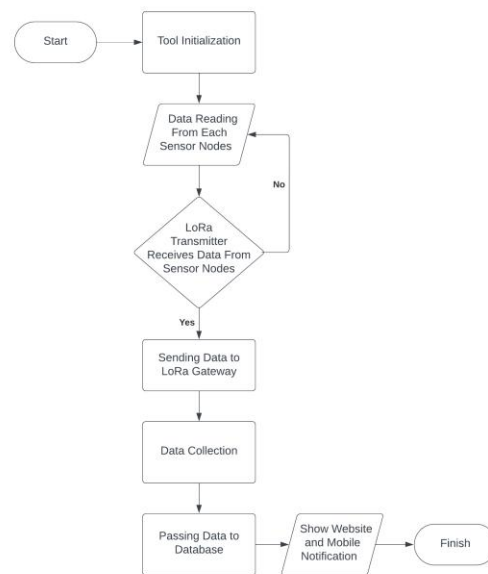


**Figure 2.** System Workflow Diagram

Table 3 documents the environmental factors (temperature, humidity, and weather) during each test. Environmental conditions such as rain, high humidity, and overcast skies can negatively affect LoRa signal propagation. Therefore, it is necessary to report these parameters to contextualize the performance results.

**Table 3.** Environmental Conditions During Tests

Distance (m)	Temperature (°C)	Humidity (%)	Weather Condition
50	28	70	Sunny
180	29	65	Partly Cloudy
300	27	75	Cloudy
340	30	80	Light Rain
440	31	85	Overcast

The table shows that the poorest performance was recorded during light rain and overcast conditions at longer distances. This suggests that adverse weather contributed to the increased packet loss and delays observed beyond 300m. By including these details, the study acknowledges external factors beyond mere distance that influence signal performance.

#### 4. Results and Discussion

In the following discussion, the author will discuss the steps for collecting data, description of data collection, data analysis, and finally data interpretation.

#### 4.1. Data Reception Range Measurement

This test is conducted by setting several specific distance ranges between the node and the gateway to evaluate the performance of LoRa communication under various conditions. The distances used in this test include 50 meters, 180 meters, 300 meters, 340 meters, and 440 meters. The selection of these distances is not done arbitrarily, but is based on the results of previous product tests. Initial test results show that in this range there is a significant variation in signal quality due to environmental factors, such as building obstacles, interference, and increasing distance. By dividing the test into several distance ranges, it is hoped that a more comprehensive analysis of the performance of the LoRa communication system can be obtained in various scenarios in the real environment.

At a distance of 50 meters, the node is placed in the KJA area located at the front of BTP Telkom. This location was chosen because it is relatively open and has good visibility to the gateway. Meanwhile, the gateway is placed at the top of the BTP Telkom building to ensure optimal signal coverage and minimize the possibility of obstruction of the communication path between the node and the gateway. With this position, it is expected that data transmission can take place without significant obstacles. An illustration of the placement of nodes and gateways in this test can be seen in figure 3.

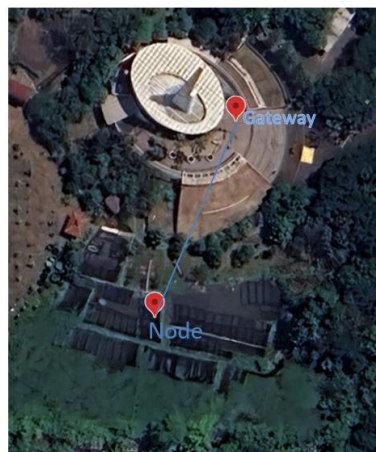


**Figure 3.** 50 Meters Distance

The data test results show that all messages sent by the node were successfully received by the gateway without any loss of data packets. This indicates that at a distance of 50 meters, communication between the node and the gateway is running very optimally. As shown in table 4, all messages sent can be received intact without any significant interference. In this test, the observed data transmission delay varied, with the highest value reaching 3 seconds and the lowest value being 1 second. This delay variation can be influenced by several factors, such as signal propagation conditions in the surrounding environment, electromagnetic interference from other devices, and the processing load on the sending and receiving devices. In addition, the results of measuring the signal quality indicator show that the RSSI value is in the range of -106 dBm to -85 dBm. This value is still categorized as quite good for LoRa communication, especially in environments with few physical obstacles. Meanwhile, the Signal-to-Noise Ratio (SNR) obtained was more than 9 dB, indicating that the received signal has very good quality with minimal interference.

**Tabel 4.** 50 Meters Distance

No	Acceptance Status	Delay (seconds)	RSSI (dBm)	SNR (dB)	No	Acceptance Status	Delay (seconds)	RSSI (dBm)	SNR (dB)
1	Success	1	-101	9	11	Success	2	-88	10
2	Success	2	-105	9	12	Success	1	-89	10
3	Success	1	-106	8	13	Success	1	-89	8
4	Success	1	-102	9	14	Success	1	-91	9
5	Success	3	-101	9	15	Success	2	-88	9

6	Success	2	-100	9	16	Success	2	-90	8
7	Success	3	-102	8	17	Success	1	-87	9
8	Success	1	-105	9	18	Success	1	-85	9
9	Success	2	-105	9	19	Success	2	-89	10
10	Success	3	-106	9	20	Success	2	-88	9

Next, testing was conducted at a distance of 180 meters to evaluate the extent to which the quality of LoRa communication remains optimal when the distance between the node and the gateway is increased. In this test, the node remains placed in the KJA area located at the front of BTP Telkom, maintaining the same position as in the previous test. Meanwhile, the gateway was moved to a higher location, namely on the 7th floor of the GKU Building, Telkom can be seen in [figure 4](#).



**Figure 4.** 180 Meters Distance

The test results at a distance of 180 meters showed that all messages sent by the node were successfully received by the gateway without any loss of data packets. This success indicates that even though the distance between the node and the gateway is further than the previous test, the LoRa communication system is still able to work optimally. The message data received by the gateway can be seen more clearly in [table 5](#), which shows that each message was successfully transmitted and processed properly. In this test, the delivery delay varied with a maximum value of 5 seconds and a minimum value of 1 second. The increase in delay compared to the test at a distance of 50 meters can be caused by several factors, such as signal propagation starting to weaken, changes in environmental conditions, and the possibility of interference from other sources. Although there was an increase in delay, this time range is still within acceptable limits for periodic data monitoring applications using LoRa.

**Tabel 5.** 180 Meters Distance

No	Acceptance Status	Delay (seconds)	RSSI (dBm)	SNR (dB)	No	Acceptance Status	Delay (seconds)	RSSI (dBm)	SNR (dB)
1	Success	1	-112	7	11	Success	2	-97	8
2	Success	3	-111	8	12	Success	3	-97	9
3	Success	5	-109	7	13	Success	2	-96	8
4	Success	1	-112	7	14	Success	1	-95	8
5	Success	4	-108	6	15	Success	3	-96	9
6	Success	5	-109	7	16	Success	2	-104	7



7	Success	3	-119	6	17	Success	2	-104	9
8	Success	2	-113	7	18	Success	1	-107	8
9	Success	3	-109	6	19	Success	2	-109	9
10	Success	5	-113	6	20	Success	3	-107	8

In addition, the signal quality indicator also changed compared to the previous test. The RSSI value obtained ranged from -112 dBm to -95 dBm, which indicates a slight decrease in signal strength due to the increase in distance and the possibility of propagation interference. Meanwhile, the SNR varies between 6 dB to 9 dB, which is still in a good enough range to ensure reliable communication. Despite the increase in delay and slight decrease in signal quality, the test results show that communication between the node and the gateway at a distance of 180 meters can still take place well and is feasible to be used in the implementation of a LoRa-based water toxicity monitoring system.

In the 300-meter test, the node was moved to the KJA area located at the back of BTP Telkom. This location was chosen to evaluate how changes in node position, especially in terms of the presence of potential obstacles around the test area, can affect the quality of LoRa communication. Meanwhile, the gateway was maintained on the 7th floor of the GKU Building to maintain consistency in testing and to see how increasing distance affects signal reception. With the increase in distance to 300 meters, there is a possibility of increased signal attenuation due to propagation effects and potential environmental interference. Therefore, the measurement in this scenario aims to analyze communication performance under more challenging conditions compared to the previous distance as seen in [figure 5](#).

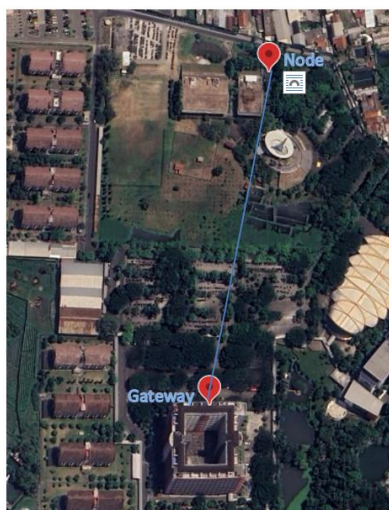


**Figure 5.** 300 Meters Distance

The test results at a distance of 300 meters showed that all messages sent by the node were successfully received by the gateway without any loss of data packets, as shown in [table 6](#). This successful reception shows that the LoRa communication system can still work well at medium distances. However, as the distance between the node and the gateway increases, there is an increase in delay in the data transmission process. The test recorded that the highest delay value reached 6 seconds, while the lowest delay value was still in the range of 1 second. In addition, signal strength measurements showed that the RSSI value experienced a significant decrease, with the lowest value reaching -120 dBm. On the other hand, the SNR also showed a fairly striking weakening, with a value that dropped by up to 2 dB. This indicates that the signal quality received by the gateway is starting to degrade, so that it can affect communication stability in more complex environmental conditions.

**Tabel 6.** 300 Meters Distance

No	Acceptance Status	Delay (seconds)	RSSI (dBm)	SNR (dB)	No	Acceptance Status	Delay (seconds)	RSSI (dBm)	SNR (dB)
1	Success	1	-119	2	11	Success	1	-114	2

2	Success	5	-111	3	12	Success	3	-113	2
3	Success	6	-119	2	13	Success	2	-109	3
4	Success	2	-112	3	14	Success	1	-111	5
5	Success	1	-115	4	15	Success	3	-109	4
6	Success	1	-120	5	16	Success	2	-109	2
7	Success	2	-119	2	17	Success	1	-111	3
8	Success	3	-113	2	18	Success	1	-113	3
9	Success	2	-119	3	19	Success	3	-107	1
10	Success	2	-113	1	20	Success	3	-111	2

At a distance of 340 meters, the gateway that was previously located on the 7th floor of the GKU Building was moved to the 5th floor of the FIT Building. Meanwhile, the node remains placed in the KJA area located at the front of BTP Telkom, as seen in [figure 6](#). The shift in the gateway location aims to analyze how changes in the physical environment, especially the presence of more building obstacles, affect data transmission performance.



**Figure 6.** 340 Meters Distance

Of the total 20 data transmission attempts conducted at a distance of 340 meters, only one attempt was successful, namely the 9th attempt, as shown in [table 7](#). However, although the data was successfully received by the gateway, there were serious obstacles in terms of delivery delays. The delay observed in this experiment reached a very high number, namely up to 50 minutes, which was much greater than the test at the previous distance. In addition, the signal quality indicator showed very poor results. The RSSI value was recorded at -134 dBm, indicating that the signal received by the gateway was at the minimum threshold and was experiencing significant attenuation. On the other hand, the SNR experienced a drastic decrease to -6 dB, indicating high interference and low signal quality that could be processed by the gateway.

**Table 7.** 340 Meters Distance

No	Acceptance Status	Delay (seconds)	RSSI (dBm)	SNR (dB)	No	Acceptance Status	Delay (seconds)	RSSI (dBm)	SNR (dB)
1	Fail	-	-	-	11	Fail	-	-	-
2	Fail	-	-	-	12	Fail	-	-	-
3	Fail	-	-	-	13	Fail	-	-	-
4	Fail	-	-	-	14	Fail	-	-	-
5	Fail	-	-	-	15	Fail	-	-	-
6	Fail	-	-	-	16	Fail	-	-	-
7	Fail	-	-	-	17	Fail	-	-	-

8	Fail	-	-	-	18	Fail	-	-	-
9	Success	50.0	-134	-6	19	Fail	-	-	-

At a distance of 440 meters, the node location is at the KJA behind BTP Telkom and the gateway location is on the 5th floor of the FIT Telkom building. The condition worsens with many reception failures as seen in the building that acts as a barrier between the node and the gateway in [figure 7](#). The shift in the gateway location aims to analyze how changes in the physical environment, especially the presence of more building obstacles, affect data transmission performance.



**Figure 7.** 440 Meters Distance

The measurement results at a distance of 440 meters, as shown in [table 8](#), show many data reception failures due to long distances and building obstacles. Out of 20 trials, only the 6th, 7th, 9th, 15th, 18th, and 20th trials were successful. Although the data was successfully received, the transmission delay was quite high, with the highest value being 15.2 seconds and the lowest being 5.3 seconds. The RSSI value ranged from -132 dBm to -122 dBm, indicating a very weak signal. Meanwhile, the SNR was recorded at only -4 dB, indicating high interference and noise.

**Tabel 8.** 440 Meters Distance

No	Acceptance Status	Delay (seconds)	RSSI (dBm)	SNR (dB)	No	Acceptance Status	Delay (seconds)	RSSI (dBm)	SNR (dB)
1	Fail	-	-	-	11	Fail	-	-	-
2	Fail	-	-	-	12	Fail	-	-	-
3	Fail	-	-	-	13	Fail	-	-	-
4	Fail	-	-	-	14	Fail	-	-	-
5	Fail	-	-	-	15	Success	15.2	-122	-1
6	Success	5.3	-127	2	16	Fail	-	-	-
7	Success	6.4	-126	1	17	Fail	-	-	-
8	Fail	-	-	-	18	Success	12.2	-125	-3
9	Success	10.2	-132	-3	19	Fail	-	-	-
10	Fail	-	-	-	20	Success	10.3	-126	-4

## 4.2. Reach Data Analysis

With the testing that has been done, the comparison between each distance has different delay, RSSI, and SNR values. The test was carried out 20 times at various ranges to get more accurate results. With the testing that has been done, a

comparison between each distance has different delay, RSSI, and SNR values. Testing was carried out 20 times at various ranges to get more accurate results. In [figure 8\(a\)](#) the graph shows the average RSSI value obtained during testing. The results of this measurement indicate that the LoRa signal weakens as the distance increases with a drastic decrease in the first 50 meters and is more stable up to 300 meters. At 340 meters, there is a sharp decrease, due to physical obstacles such as buildings that cause Nlos. A slight increase at 440 meters is caused by the placement which is still considered acceptable, where the condition changes to nLoS.

In [figure 8\(b\)](#) the graph shows the average Delay value obtained during the test. The graph shows the relationship between distance and delay in LoRa communication. At first, the delay increases gradually up to a distance of 300 meters, but is still in a relatively small range. However, at 340 meters there is a very high delay spike, reaching almost 50 minutes, which is caused by signal interference, physical obstacles, interference, or the effective range limit of LoRa. After that, the delay decreases again at a distance of 440 meters, although it is still higher than the previous distance.

[Table 9](#) provides a consolidated summary of system performance across various test distances, reflecting the average delay, RSSI, SNR, and successful data transmission rates. It clearly demonstrates that performance begins to degrade notably beyond 300 meters. At 340 meters, the metrics fall sharply due to NLoS interference, making this distance the least effective for reliable data transfer. The 440-meter test yields slightly better outcomes due to its nLoS configuration. From this table, it becomes clear that while the average delay remains acceptable up to 300m, the maximum delay and packet loss spike dramatically at 340m and 440m. Such insights help stakeholders determine acceptable operational ranges and implement mitigation strategies such as repeaters or better antenna placement. This table enhances the clarity of data trends and supports the graphical analysis presented in [figure 8](#).

**Table 9.** Average Performance of LoRa Communication Parameters by Distance

Distance (m)	Avg Delay (s)	Min Delay (s)	Max Delay (s)	Avg RSSI (dBm)	Min RSSI (dBm)	Max RSSI (dBm)	Packet Loss (%)
50	1.9	1.0	3.0	-94.7	-106	-85	0
180	2.7	1.0	5.0	-104.3	-119	-95	0
300	2.5	1.0	6.0	-113.4	-120	-107	0
340	50.0	50.0	50.0	-134.0	-134	-134	95
440	9.6	5.3	15.2	-126.8	-132	-122	70

In [figure 8\(c\)](#) the graph shows the average SNR values obtained during the test. The graph shows the relationship between distance and SNR in LoRa communication. Initially, the SNR is around 10 dB and remains stable up to 180 meters. However, after passing this distance, the SNR begins to decrease significantly, especially after a distance of 300 meters, until it reaches a negative value at a distance of 340 indicating that at this point there are obstacles that cause significant interference. In addition, at a distance of 440 meters, although there are still obstacles, the condition changes to nLoS, which means that the signal propagation path is slightly more open than the previous point.

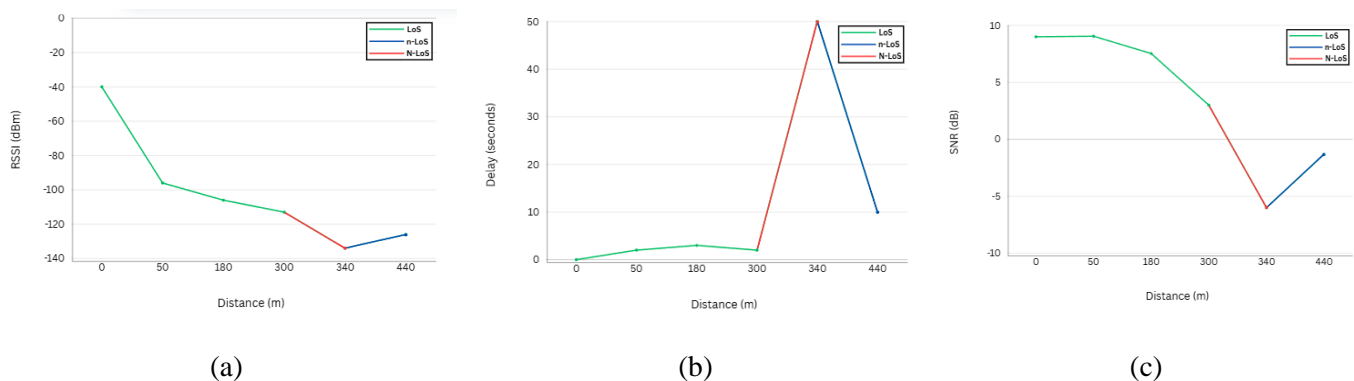


**Figure 8.** Average RSSI, Delay and SNR graphs

Based on the test results that have been carried out, all the graphs obtained show a fairly significant trend of change at a certain distance. Specifically, at a distance of 340 meters, the graph experiences a fairly drastic decline. This is because the amount of data that appears at that point is very small, where statistically only one data is successfully recorded. This condition indicates an anomaly in the data distribution at that distance, which is caused by building obstacles that affect the LoRa communication process. Furthermore, at a distance of 440 meters, the graph actually increases again. This increase occurs because the amount of data successfully received increases to six data in the test range. This anomaly indicates that at a certain distance, the communication system experiences significant fluctuations in terms of the amount of data received, which can have implications for the overall performance of the LoRa network. As a result of the drastic decline at a distance of 340 meters and a sudden increase at a distance of 440 meters, the graph shows a fairly sharp change in pattern, reflecting inconsistencies in data reception at that distance range.

In LoRa communication, signal range is affected by factors such as delay, RSSI, and SNR, which determine whether data can be received well, intermittently, or even completely disconnected. One of the main factors affecting signal quality is the Fresnel Zone, which plays a role in maintaining the stability and strength of signal transmission. The Fresnel Zone is an elliptical area located between the transmitter and receiver. At a distance of 50 meters to 300 meters is the Fresnel Zone LoS [39]. Where the line of sight is visible between the sending station and the receiving station facing each other without any obstacles between them. While the fresnel zone is one of a series of areas or ellipsoidal spaces around and between the transmitter and receiver. In addition to LoS, there is something called nLoS where the visible view still exists, but the fresnel zone is blocked by certain objects [40], such as a range test with a distance of 440 meters, so that data can still be sent but the signal between the receiver and sender is disconnected. The last Fresnel Zone, namely Non Line of Sight is a condition where the view of the eye and the fresnel zone are blocked by objects as a whole [40], [41], such as in a range test with a distance of 340 meters, so that the data has experienced reception interference and the possibility of a distance of 340 meters cannot be served by the system if this happens then the connection will be disconnected completely.

### 4.3. LoS Measurement Based on Power Difference (dB)

Testing was conducted by comparing the variation of transmit power in the range of 2 dB to 20 dB, with a gradual increase in even multiples as seen in figure 9(a) and figure 9(b). This test uses data obtained under LOS conditions with three different measurement points, namely at a distance of 50 meters, 180 meters, and 300 meters. Analysis was conducted to evaluate how changes in transmit power affect communication quality and signal reception stability at each distance. Figure 9(a) shows the relationship between transmit power and signal reception (RSSI) at distances of 50 meters, 180 meters, and 300 meters under LOS conditions. The higher the transmit power, the RSSI increases (stronger), especially at closer distances. However, at a distance of 300 meters, the increase in RSSI is not always consistent, possibly due to signal attenuation or interference.

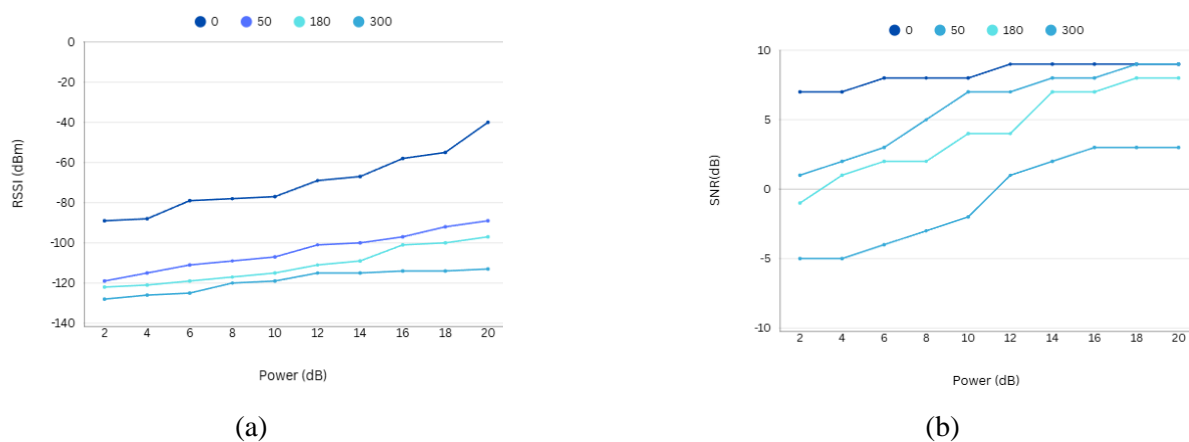


**Figure 9.** Difference between Power and RSSI and SNR

In figure 9(b) the graph shows the relationship between transmit power (Power) and SNR at distances of 50m, 180m, and 300m under LOS conditions. In general, increasing transmit power causes an increase in SNR, which means improved signal quality. At closer distances (50m), the SNR is higher compared to longer distances (180m and 300m).



However, at a distance of 300m, the SNR is lower and even negative at low transmit power, indicating a weaker signal and more affected by noise.

#### 4.4. Functional Protocol Results

The functional results of the LoRa communication protocol tested in this study aim to evaluate whether the LoRa communication system applied to the KJA can operate optimally and in accordance with the needs of monitoring the aquatic environment. Testing was carried out 20 times with various distance variations to measure effectiveness in the process of sending and receiving data. In addition, this test also aims to analyze changes in water conditions that occur over a certain period of time, so that the system can provide accurate and real-time information related to the observed environmental parameters. Based on the research design, the LoRa node sensor and LoRa gateway devices were placed at two different points, namely on the KJA located in front of BTP Telkom and the KJA located behind BTP Telkom.

The distance between the two points is 180 meters and 300 meters, which were chosen to observe the extent of the LoRa communication range in aquatic environmental conditions with various potential obstacles that may occur using solar panels for long-term operations. Based on the results of the trials that have been carried out and displayed in [table 10](#), it can be concluded that all the main functions in this system have run according to the designed specifications. The implementation of hardware and software in this communication system shows that the protocol used is able to optimize the sending and receiving of data in the LoRa network.

**Tabel 10.** Functional Overview of the LoRa Communication System

System Component	Function Description	Test Outcome
Sensor Node (ESP32 + Sensors)	Collecting environmental data	Successful
LoRa Node	Transmitting data to the gateway	Successful
LoRa Gateway	Forwarding data to the database	Successful
Web Dashboard	Visualizing data in real-time	Successful
Notification System	Alerting users on critical risk conditions	Successful

The functional test in the [table 11](#) expands on the previous summary by showing the number of trials, success rates, and response times for each component. Such detail confirms the robustness and reliability of each subsystem in the communication chain. It also highlights the weakest links that might require further optimization. For instance, the LoRa Node and Gateway have slightly lower success rates (95%) compared to the Sensor Node and Dashboard (100%), indicating minor but noteworthy communication challenges in the wireless segment. This level of detail is essential for diagnosing performance bottlenecks and prioritizing improvements.

**Table 11.** Functional Test Detailed Results

Component	Function	No. of Trials	Success Rate (%)	Avg Response Time (s)
Sensor Node	Data collection	20	100	0.5
LoRa Node	Data transmission	20	95	1.0
LoRa Gateway	Data forwarding	20	95	1.2
Web Dashboard	Data visualization	20	100	0.8
Notification System	Alert generation	20	100	1.5

The risk level calculation formula is designed to provide a quantitative assessment of water quality based on three critical parameters: temperature, pH, and dissolved oxygen. Each of these factors influences the survival and health of fish in floating net cages. By assigning specific weights to each parameter, the formula reflects the relative importance of each factor to aquatic life. Temperature influences metabolic rates, pH affects enzyme activity and osmotic balance, while dissolved oxygen is directly related to respiration. The absolute deviation of pH from the neutral optimal value (7.5) and the deficit of DO from its optimal value (8 mg/L) are both penalized because such deviations can indicate increasing toxicity risk.

$$R = w_T \cdot T + w_{pH} \cdot |pH - 7.5| + w_{DO} \cdot (8 - DO) \quad (4)$$

$R$  = risk score (higher means more dangerous);  $T$  = temperature;  $pH$  = pH of water;  $DO$  = dissolved oxygen (mg/L);  $w_T, w_{pH}, w_{DO}$  = *weight for each parameter*; Reference values:  $pH$  optimal = 7.5,  $DO$  optimal = 8 mg/L

The weighted risk score  $R$  enables the dashboard to categorize conditions into distinct statuses (Safe, Alert, Danger), facilitating easy interpretation for fish farmers. The table complements the formula by translating numerical scores into actionable categories, providing clarity on what farmers should do at each level. For example, a score below 50 means conditions are optimal, whereas scores above 80 demand immediate mitigation measures such as oxygenation, water exchange, or reducing stocking density. The color-coded indicators (green, yellow, orange, red) also ensure that users can quickly assess conditions at a glance.

By enriching the table with intermediate Alert categories (low and high), the system offers finer granularity, enabling more proactive management. Instead of binary “Safe” vs. “Danger,” users are informed about the escalating risk, helping them prepare in advance before a crisis emerges. This design aligns with the goal of early warning systems, giving farmers sufficient time to act, thus minimizing losses and maintaining ecological balance.

Moreover, the explicit use of a formula ensures transparency and reproducibility. Stakeholders can adjust the weights  $w_T, w_{pH}, w_{DO}$  based on species-specific sensitivities or local environmental contexts. For instance, if the cultivated species is highly sensitive to pH fluctuations,  $pH$  can be increased, making the system more adaptive. This flexibility is crucial in making the system not only effective but also customizable for various aquaculture scenarios, thereby enhancing its value as a decision-support tool.

#### 4.5. Dashboard and Database Functional Testing

This test aims to ensure that the dashboard can be connected to the ESP32 via a database and display data from sensors, including air temperature, pH, DO, and risk levels. The testing process was carried out using a laptop capable of displaying data in real time. In addition, the dashboard is equipped with a button that allows users to combine environmental conditions and receive early warnings as alarms for farmers in floating net cages. The data stored in Firebase comes from sensors on the LoRa Node Sensor, which are then sent to the LoRa Gateway. Furthermore, the data stored in the database will be saved to the dashboard directly. [Figure 10](#) shows the Firebase display that stores data on air temperature, pH, DO, risk level, SNR, and RSSI. Data from Firebase is then displayed on the dashboard, as seen in [figure 11](#). On the main dashboard display, there are several sensor panels that display air quality parameters visually, such as DO, pH, risk level, and air temperature. Each panel is equipped with a graph showing changes in values over time, as well as information about the current sensor value and average measurement. Status sensors are also displayed to ensure that the device is functioning properly. On the right side of the dashboard, there is a system time indicator, a connection status sensor that shows whether it is Online or Offline, and an alarm that provides a warning if there are parameters that are outside the safe limit. These warnings are marked with the words "Safe!" in green for safe conditions, "Alert" for moderate conditions, and "Danger!" in red for high conditions. The safe limit is determined based on the risk value calculated from the average air temperature, pH, and DO data. If the risk value is less than 50, the alarm will display the Safe status; if it is in the range of 50 to 80, the alarm will show the Alert status; and if the risk value exceeds 80, the Danger status will be displayed. To use this dashboard, users need to ensure that the sensor device is active and properly connected. After that, users can combine the displayed parameter values to find out the condition of the aquatic environment. If the Danger! warning appears, users are advised to immediately check and take the necessary actions to avoid risks to the aquatic ecosystem and the sustainability of fish farming.

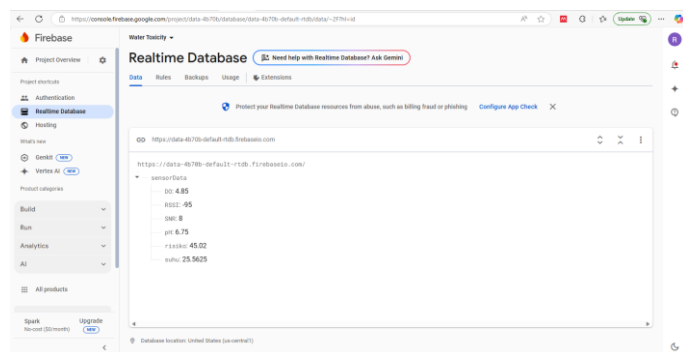


**Figure 10.** Views in Firebase

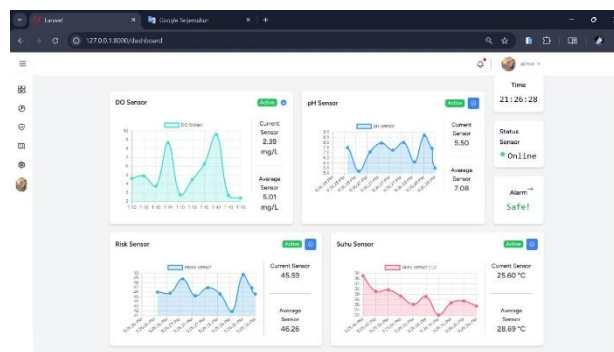


**Figure 11.** Views in Dashboard

## 5. Conclusion

After conducting a series of studies and tests on the LoRa communication system applied to KJA, it can be concluded that the optimal placement of two LoRa sensor node points is at a distance of 180 meters and 300 meters. At this distance, communication between the LoRa sensor node and the LoRa gateway can run well in LOS conditions, allowing for a more stable and efficient data sending and receiving process. The test results show that although this communication system can operate optimally, there are several factors that affect the quality of data reception, including the RSSI, Delay, and SNR values. Overall, the implementation of the LoRa communication system in this study has shown good performance and can be used for monitoring water quality in KJA. However, to improve the efficiency and consistency of data transmission, several adjustments are needed, such as antenna optimization, transmission power adjustment, or the use of interference mitigation techniques so that the system can work more stably in various environmental conditions. With further development, this system has great potential in supporting real-time water quality monitoring, which can ultimately improve the efficiency and sustainability of KJA management.

## 6. Declarations

### 6.1. Author Contributions

Conceptualization: R., I.D.I., M.F.R., and S.S.M.; Methodology: S.S.M.; Software: R.; Validation: R., S.S.M., and M.F.R.; Formal Analysis: R., S.S.M., and M.F.R.; Investigation: R.; Resources: S.S.M.; Data Curation: S.S.M.; Writing Original Draft Preparation: R., S.S.M., and M.F.R.; Writing Review and Editing: S.S.M., R., and M.F.R.; Visualization: R.; All authors have read and agreed to the published version of the manuscript.

### 6.2. Data Availability Statement

The data presented in this study are available on request from the corresponding author.

### 6.3. Funding

The authors received no financial support for the research, authorship, and/or publication of this article.

### 6.4. Institutional Review Board Statement

Not applicable.

### 6.5. Informed Consent Statement

Not applicable.

### 6.6. Declaration of Competing Interest

The authors declare that they have no known competing financial interests or personal relationships that could have appeared to influence the work reported in this paper.

## References

- [1] S. S. Adhawati and St. M. Mansyur, "Potential and Projection of GRDP Value in the Fisheries Sector of South Sulawesi Province," *Journal of Marine and Fisheries Socio-Economics*, vol. 18, no. 1, pp. 133-145, Dec. 2023, doi: 10.15578/jsekp.v18i2.12280.
- [2] F. Bernal-Higueta, M. Acosta-Coll, F. Ballester-Merelo, and E. De-la-Hoz-Franco, "Implementation of information and communication technologies to increase sustainable productivity in freshwater finfish aquaculture – A review," *Journal of Cleaner Production*, vol. 408, no. July, pp. 1020, Jul. 2023, Elsevier Ltd. doi: 10.1016/j.jclepro.2023.137124.
- [3] T. Adiono, F. Albertha, R. Mulyawan, and E. Sumiarsih, "Power Management Design for Floating Net Cages Water Quality Monitoring System," in *2021 International Conference on Electrical Engineering and Informatics (ICEEI)*, IEEE, Oct. 2021, pp. 1–5. doi: 10.1109/ICEEI52609.2021.9611116.
- [4] D. Hidayati, S. A. Dalimunthe, and I. A. P. Putri, "Socio-economic Vulnerability and Benefits to the Community Associated with Floating Fish Cages in the Jatiluhur Reservoir," *The Water-Energy-Food Nexus*, vol. 2018, no. 1, pp. 245–260, 2018. doi: 10.1007/978-981-10-7383-0\_17.
- [5] I. Gumilar, R. M. S. Rasyid, Y. Andriani, and I. Maulina, "Profile of Double Layer Floating Net Cage Fish Farming Business in Saguling Reservoir (Case Study of Bongas Village, Cililin District, West Bandung Regency)," *Journal of Fisheries Unram*, vol. 15, no. 1, pp. 285–298, Feb. 2025, doi: 10.29303/jp.v15i1.1358.
- [6] D. Hermanto, D. Stiawan, B. Y. Suprpto, E. Permata, and E. P. Widiyanto, "New Approach Monitoring System with ESP32 and MQTT for the Best Position of the Floating Net Cage," in *2023 10th International Conference on Electrical Engineering, Computer Science and Informatics (EECSI)*, IEEE, vol. 2023, no. Sep., pp. 139–144, 2023. doi: 10.1109/EECSI59885.2023.10295802.
- [7] M. T. Dokulil and K. Teubner, "Eutrophication and Climate Change: Present Situation and Future Scenarios," in *Eutrophication: causes, consequences and control*, Springer Netherlands, vol. 2010, no. 1, pp. 1–16, 2010. doi: 10.1007/978-90-481-9625-8\_1.
- [8] H. Yemendzhiev, P. Zlateva, and V. Nenov, "Water Safety and Toxicity Assessment Using Real Time Sensor Measurements and Fuzzy Logic Data Processing," in *Lecture Notes in Networks and Systems*, Springer Science and Business Media Deutschland GmbH, 2023, pp. 39–46. doi: 10.1007/978-3-031-31069-0\_5.
- [9] A. C. Martelo, M. Clavero, C. Caleta, and M. Hermoso, "Factors related to fish kill events in Mediterranean reservoirs," *Science of the Total Environment*, vol. 677, no. 1, pp. 94-103, Sep. 2019, doi: 10.1016/j.scitotenv.2019.04.346.
- [10] A. Bouzid, H. Chlaida, Y. Mhamdi, M. Mabrouki, and R. A. Houhamdi, "Factors associated with fish mass mortality events in North African freshwater ecosystems, Morocco as a case study," *Science of the Total Environment*, vol. 940, no. 1, pp. 15-35, Jan. 2025, doi: 10.1016/j.scitotenv.2024.156655.
- [11] I. D. Irawati, D. N. Ramadan, and S. Hadiyoso, "Web-based Water Quality Parameter Monitoring for Bok Coy Hydroponics using Multi Sensors," *Journal of Electrical Engineering Design*, vol. 18, no. 3, pp. 1-12, Sep. 2022, doi: 10.17529/jre.v18i3.26017.
- [12] Y. Wang, C. Qi, and H. Pan, "Design of remote monitoring system for aquaculture cages based on 3G networks and ARM-Android embedded system," in *Procedia Engineering*, vol. 2012, no. 1, pp. 79–83, 2012. doi: 10.1016/j.proeng.2011.12.672.
- [13] T. Abinaya, J. Ishwarya, and M. Maheswari, "A Novel Methodology for Monitoring and Controlling of Water Quality in Aquaculture using Internet of Things (IoT)," in *2019 International Conference on Computer Communication and Informatics, ICCCI 2019*, Institute of Electrical and Electronics Engineers Inc., vol. 2019, no. Jan., pp. 1-7, 2019. doi: 10.1109/ICCCI.2019.8821988.
- [14] M. Roslee *et al.*, "Internet of Things: Agriculture Precision Monitoring System based on Low Power Wide Area Network," *WSEAS Transactions on Electronics*, vol. 15, no. 1, pp. 35–46, 2024, doi: 10.37394/232017.2024.15.5.
- [15] K. Mekki, E. Bajic, F. Chaxel, and F. Meyer, "A comparative study of LPWAN technologies for large-scale IoT deployment," *ICT Express*, vol. 5, no. 1, pp. 1–7, Mar. 2019, doi: 10.1016/j.ict.2017.12.005.
- [16] R. Gao, M. Jiang, and Z. Zhu, "Low-power wireless sensor design for LoRa-based distributed energy harvesting system," *Energy Reports*, vol. 9, pp. 35–40, Oct. 2023, doi: 10.1016/j.egy.2023.08.056.
- [17] H. Tahaei, H. Ruan, P. Sun, Y. Dong, and Z. Fang, "An Overview of LoRa Localization Technologies," *Computers, Materials and Continua*, vol. 82, no. 2, pp. 1645–1680, 2025, doi: 10.32604/cmc.2024.059746.
- [18] S. Devalal and A. Karthikeyan, "LoRa Technology - An Overview," in *2018 Second International Conference on Electronics, Communication and Aerospace Technology (ICECA)*, IEEE, Mar. 2018, pp. 284–290. doi: 10.1109/ICECA.2018.8474715.

- 
- [19] N. Jovalekic, V. Drndarevic, E. Pietrosevoli, I. Darby, and M. Zennaro, "Experimental Study of LoRa Transmission over Seawater," *Sensors (Basel)*, vol. 18, no. 9, Sep. 2018, doi: 10.3390/S18092853.
- [20] H. A. Khaderani, A. Agusdian, and Iskandar, "Development of Data Compression Techniques for IoT Data Transmission in Isolated Aquaculture Using LoRa Through LoRaWAN Gateway Antares Telkom," in *2024 18th International Conference on Telecommunication Systems, Services, and Applications (TSSA)*, IEEE, vol. 2024, no. Oct., pp. 1–5, 2024. doi: 10.1109/TSSA63730.2024.10863914.
- [21] Y. Sari, "Internet of Things for Water Quality Monitoring System in Catfish Ponds of TDR Sultan Adam Banjarmasin Farmers," *Journal of Superior Wetland Innovation Service*, vol. 3, no. Augustus, pp. 203–213, 2023, doi: 10.20527/ilung.v3i1.
- [22] A. F. Zulkarnain, A. T. E. Suryo, and M. Mahrudin, "Design of a Patin Fish Farming Monitoring System Based on LoRa Protocol Using Fuzzy Logic Method," *Bulletin of Professional Engineers*, vol. 7, no. 1, pp. 13–22, Feb. 2024, doi: 10.20527/BPI.V7I1.230.
- [23] R. O. Andrade and S. G. Yoo, "A Comprehensive Study of the Use of LoRa in the Development of Smart Cities," *Applied Sciences*, vol. 9, no. 22, pp. 4753–4768, Nov. 2019, doi: 10.3390/app9224753.
- [24] N. J. B. Florita, A. N. M. Senatin, A. M. A. Zabala, and W. M. Tan, "Opportunistic LoRa-based gateways for delay-tolerant sensor data collection in urban settings," *Comput Commun*, vol. 154, no. 1, pp. 410–432, Mar. 2020, doi: 10.1016/j.comcom.2020.02.066.
- [25] G. Kaur, V. Balyan, and S. H. Gupta, "Experimental analysis of low-duty cycle campus deployed IoT network using LoRa technology," *Results in Engineering*, vol. 23, no. 1, pp. 10–24, Sep. 2024, doi: 10.1016/j.rineng.2024.102844.
- [26] M. González-Palacio *et al.*, "Novel RSSI-Based localization in LoRaWAN using probability density estimation similarity-based techniques," *Internet of Things*, vol. 31, no. 1, pp. 10–51, May 2025, doi: 10.1016/j.iot.2025.101551.
- [27] K. Abdulameer, Z. N. Khudhair, H. F. Mohsin, K. A. Kadhim, and Z. N. Khudhier, "Study and performance analysis of received signal strength indicator (RSSI) in wireless communication systems," *Article in International Journal of Engineering and Technology*, vol. 6, no. 4, pp. 195–200, 2017, doi: 10.14419/ijet.v6i4.29558.
- [28] M. A. Kamal, M. M. Alam, A. A. B. Sajak, and M. M. Su'ud, "SNR and RSSI Based an Optimized Machine Learning Based Indoor Localization Approach: Multistory Round Building Scenario over LoRa Network," *Computers, Materials and Continua*, vol. 80, no. 2, pp. 1927–1945, 2024, doi: 10.32604/cmc.2024.052169.
- [29] A. D. Haq, I. Santoso, A. Ajulian, and Z. Macrina, "Estimation of Signal to Noise Ratio (SNR) Using the Correlation Method," *Scientific Journal of Electrical Engineering*, vol. 1, no. 4, pp. 326–332, Dec. 2012, doi: 10.14710/TRANSIENT.V1I4.326-332.
- [30] F. Fahmi, Y. Salim, and R. Satra, "Quality of Service Analysis Using Delay, Packet Loss, Jitter, and Mean Opinion Score in Voice Over IP," *Proceedings of the National Seminar on Computer Science and Information Technology*, vol. 3, no. 2, 2018.
- [31] C.-C. Wei, S.-T. Chen, and P.-Y. Su, "Image Transmission Using LoRa Technology with Various Spreading Factors," in *2019 2nd World Symposium on Communication Engineering (WSCE)*, IEEE, vol. 2019, no. Dec., pp. 48–52. doi: 10.1109/WSCE49000.2019.9041044.
- [32] D. Zorbas, "Downlink Spreading Factor selection in LoRaWAN," *Comput Commun*, vol. 215, no. 1, pp. 112–119, Feb. 2024, doi: 10.1016/j.comcom.2023.12.013.
- [33] H. Y. Huang, C. M. Liang, and W. M. Chiu, "1-99% input duty 50% output duty cycle corrector," in *Proceedings - IEEE International Symposium on Circuits and Systems*, vol. 2006, no. 1, pp. 4175–4178. doi: 10.1109/iscas.2006.1693549.
- [34] Z. Chen, A. Liu, Z. Li, Y. June Choi, and J. Li, "Distributed duty cycle control for delay improvement in wireless sensor networks," *Peer Peer Netw Appl*, vol. 10, no. 1, pp. 559–578, May 2017, doi: 10.1007/s12083-016-0501-0.
- [35] L. Angrisani, P. Arpaia, F. Bonavolonta, M. Conti, and A. Liccardo, "LoRa protocol performance assessment in critical noise conditions," in *RTSI 2017 - IEEE 3rd International Forum on Research and Technologies for Society and Industry, Conference Proceedings*, Institute of Electrical and Electronics Engineers Inc., vol. 2017, no. Oct., pp. 1–7, 2017. doi: 10.1109/RTSI.2017.8065952.
- [36] Y.-H. Chang, F.-C. Wu, and H.-W. Lin, "Design and Implementation of ESP32-Based Edge Computing for Object Detection," *Sensors*, vol. 25, no. 6, art. no. 1656, pp. 120, 2025, doi: 10.3390/s25061656.
- [37] A. A. Taha, M. F. Feteiha, and W. Abdul, "Performance Evaluation for LoRa Transceiver," *International Journal of Computer Science and Software Engineering*, vol. 8, no. 2, pp. 25–39, Feb. 2019.



- [38] N. Zhu, Y. Xia, Y. Liu, C. Zang, H. Deng, and Z. Ma, "Temperature and humidity monitoring system for bulk grain container based on LoRa wireless technology," in *Lecture Notes in Computer Science (including subseries Lecture Notes in Artificial Intelligence and Lecture Notes in Bioinformatics)*, Springer Verlag, vol. 2018, no. 1, pp. 102–110. doi: 10.1007/978-3-030-00021-9\_10.
- [39] P. E. Brown, K. Czapiga, A. Jotshi, Y. Kanza, V. Kounev, and P. Suresh, "Planning Wireless Backhaul Links by Testing Line of Sight and Fresnel Zone Clearance," *ACM Transactions on Spatial Algorithms and Systems*, vol. 9, no. Jan., pp. 1-7, 2023, doi: 10.1145/3517382.
- [40] V. Díez, "Reliability evaluation of point-to-point links based on IEEE 802.15.4 physical layer for Industrial Wireless Sensor Networks," *Computers & Electrical Engineering*, vol. 86, no. May, pp. 10-38, May 2020, doi: 10.1016/j.compeleceng.2020.106738.
- [41] M. N. A. Zakaria, A. N. Ahmed, M. Abdul Malek, A. H. Birima, M. M. H. Khan, M. Sherif, and A. Elshafie, "Exploring machine learning algorithms for accurate water level forecasting in Muda River, Malaysia," *Heliyon*, vol. 9, no. 7, pp. 1-21, 2023, doi: 10.1016/j.heliyon.2023.e17689.